Vehicle Model Aided Inertial Navigation for a UAV using Low-cost Sensors

Mitch Bryson and Salah Sukkarieh
ARC Centre of Excellence in Autonomous Systems
University of Sydney
NSW 2006, Australia
m.bryson,salah@acfr.usyd.edu.au

Abstract

This paper considers two different methods of using a dynamic vehicle model in order to aid pose estimates provided by an Inertial Navigation System (INS) for a Un-manned Aerial Vehicle (UAV). We consider low-cost inertial sensors in which errors from sensor noise, bias and scale-factor errors cause a significant growth in pose estimate errors when the navigation system is un-aided by external positioning information such as from GPS or terrain observations. It is shown that an accurate dynamic vehicle model can considerably reduce the error growth in vehicle pose estimates by enhancing the observability of the inertial sensor error sources. Furthermore we analyse the effectiveness of using the vehicle model information given that there are errors in the vehicle model.

1 Introduction

Inertial navigation has commonly been used as a means of localisation for various autonomous vehicles including land, underwater and aerial vehicles. The disadvantage in the use of an Inertial Navigation System (INS), particularly when using low-cost sensors, is due to the error growth in pose estimates due to the dead-reckoning nature of the sensor. Traditionally external sensors such as GPS [Sukkarieh et al., 1999; Meyer-Hilberg and Jacob, 1994; Yang et al., 2000] or vision/radar (terrain-aided/beacon-based navigation) [Bar-Itzhack, 1978; Kim and Sukkarieh, 2003] have been used to aid the solution of the inertial navigator, thus constraining the errors in pose estimates. These external sensors have several practical disadvantages mainly relating to a reliance on external information, such as reception of satellite transmissions or reliably observable terrain features. One source of information that can be used to aid in the localisation of the vehicle, without the need for external sensing, is that from knowledge or beliefs of the vehicle's motion. Such information can be represented in two ways:

1. **Vehicle Model Constraints** - specific constraints on the pose of the vehicle i.e. a wheeled vehicle's sideways velocity will be zero.
2. **Vehicle Dynamic Modelling** - motion model of the vehicle given a history of the vehicle pose, control inputs and external forces acting on the vehicle.

The aiding of the inertial navigator with vehicle model information has been demonstrated in the past through the use of vehicle dynamic equations [Koifman and Bar-Itzhack, 1999; Ma et al., 2003] and vehicle model constraints [Dissanayake et al., 2001]. In these papers, it is shown that the major value in the use of a vehicle model is that it enhances the observability of the sources of error in the inertial navigation system. In this paper, we contribute further to the understanding of the value of dynamic vehicle model aiding by comparing two different methods of using of a six-degree of freedom dynamic Flight Vehicle Model (FVM) to aid in estimating the errors in the inertial navigation solution for an Un-manned Aerial Vehicle (UAV) using low-cost inertial sensors. The first method involves comparing and correcting for the velocity and attitude of the aircraft as predicted by both the INS and FVM. The second method uses the FVM predicted aircraft acceleration and rotation rates in order to provide direct online calibration of the IMU. We look at the effectiveness of each method given that there are parameter errors in the FVM, hinting towards the relative advantages and disadvantages of each approach when applied to a real UAV navigation problem.

In Section 2, we present a general FVM for a UAV and describe the methods of using the model to aid the inertial navigator. Section 3 describes a simulated scenario in which a UAV using a GPS aided INS loses satellite transmission mid-flight, after which vehicle model aiding is used to constrain the aircraft's pose estimate drift. In Section 4 we present simulation results of using two different methods for FVM aided INS. A discussion of the results, conclusions and future work are provided in

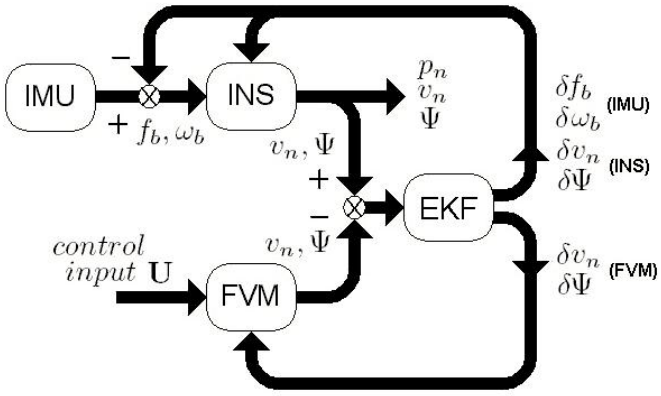

Figure 1: INS/FVM Configuration 1 - Velocity and Attitude Aiding

Section 5.

2 System Description

Figures (1) and (2) illustrate two different methods for aiding the INS using the dynamic vehicle model. In both configurations, the INS computes the position, velocity and Euler angles of the aircraft by integrating the inertial sensor readings of acceleration and rotation rates of the vehicle provided by an on-board Inertial Measuring Unit (IMU). In the first configuration, the vehicle model computes the velocity and Euler angles of the aircraft using the aircraft control inputs. An extended Kalman filter (EKF) is then used to compute the errors in both the INS and FVM from an observation of the differences between the INS and FVM computed velocity and Euler angles. In the second configuration, the FVM is used to compute the acceleration and rotation rates of the aircraft from control inputs. The inputs into the extended Kalman filter in this case are the differences between the acceleration and rotation rates computed by the FVM and those read from the inertial sensors. The extended Kalman filter is then used to estimate the errors in the inertial sensors and in the FVM accelerations and rotation rates which are then used to correct the inertial sensors and FVM accordingly.

2.1 Inertial Navigation System

The position (p_n), velocity (v_n) and Euler angles (Ψ) of the aircraft, referenced in the frame $n = [N, E, D]$ (North, East, Down) are computed as follows:

$$\dot{p_n} = v_n \quad (1)$$

$$\dot{v_n} = C_b^n f_b + g_n \quad (2)$$

$$\dot{\Psi} = E_b^n \omega_b \quad (3)$$

where g_n is the acceleration due to gravity acting on the vehicle, f_b is the body axes accelerations read by the accelerometers and ω_b is the aircraft rotation rates as read by the gyros. C_b^n and E_b^n are the body to navigation frame transformation matrix and rotation rate transformation matrix respectively as given below:

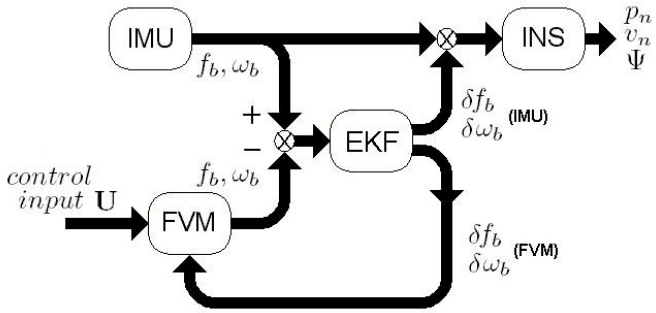

Figure 2: INS/FVM Configuration 2 - Acceleration and Rotation Rate Aiding

$$C_b^n = \begin{bmatrix} c_\psi c_\theta & c_\psi s_\theta s_\phi - s_\psi c_\phi & c_\psi s_\theta c_\phi + s_\psi s_\phi \\ s_\psi c_\theta & s_\psi s_\theta s_\phi + c_\psi c_\phi & s_\psi s_\theta c_\phi - c_\psi s_\phi \\ -s_\theta & c_\theta s_\phi & c_\theta c_\phi \end{bmatrix} \quad (4)$$

$$E_b^n = \begin{bmatrix} 1 & s_\phi t_\theta & c_\phi t_\theta \\ 0 & c_\phi & -s_\phi \\ 0 & s_\phi sec_\theta & c_\phi sec_\theta \end{bmatrix} \quad (5)$$

where $s_{(.)}$, $c_{(.)}$ and $t_{(.)}$ represent sin(.), cos(.) and tan(.) respectively and $\Psi = [\phi, \theta, \psi]$ are the Euler angles.

2.2 Flight Vehicle Dynamic Model

The FVM is made up of a set of dynamic equations that predict the values of the vehicle state $\hat{x}_v = [p, v, \Psi, \omega_b]$ composed of the vehicle's position, velocity, Euler angles and rotation rates using the aircraft control inputs which are assumed known from the aircraft's control system.

Flight Vehicle Dynamic Model Equations

Figure (3) illustrates the relationship between the relevant aircraft frames of reference. The motion of a flight vehicle can be described by the six-degree of freedom equations of motion where the forces and moments acting on the vehicle are a function of the vehicle's current position, velocity, Euler angles and rotation rates. The equations of motion are as follows:

$$\dot{u} = rv - qw + g_x + (F_x/m) \quad (6)$$

$$\dot{v} = pw - ru + g_y + (F_y/m) \quad (7)$$

$$\dot{w} = qu - pv + g_z + (F_z/m) \quad (8)$$

$$\dot{p} = C_3 pq + C_4 qr + C_1 l + C_2 N \quad (9)$$

$$\dot{q} = C_7 pr - C_6(p^2 - r^2) + C_5 M \quad (10)$$

$$\dot{r} = C_9 pq - C_3 qr + C_2 l + C_8 N \quad (11)$$

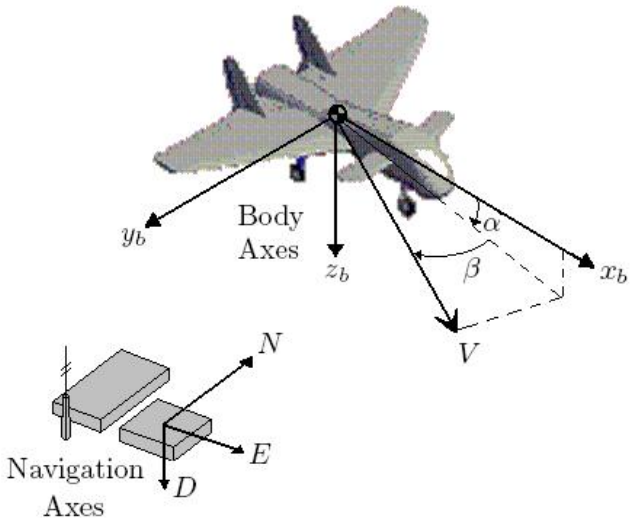

Figure 3: Aircraft Frames of Reference

where $v_b = [u, v, w]$ are the aircraft body axes velocity components, $\omega_b = [p, q, r]$ are the aircraft body axes rotation rates, F_x, F_y, F_z and l, M, N are the total force and moment components acting on the aircraft, referenced to the body axes, g_x, g_y, g_z are components of gravitational acceleration acting on the aircraft, referenced to the body axes and m is the total mass of the aircraft. The coefficients C_{0-9} are given by the following equations:

$$C_0 = I_{xx}I_{zz} - I_{xz}^2 \quad (12)$$
$$C_1 = \frac{I_{zz}}{C_0} \quad (13)$$
$$C_2 = \frac{I_{xz}}{C_0} \quad (14)$$
$$C_3 = C_2(I_{xx} - I_{yy} + I_{zz}) \quad (15)$$
$$C_4 = C_1(I_{yy} - I_{zz}) - C_2 I_{xz} \quad (16)$$
$$C_5 = \frac{1}{I_{yy}} \quad (17)$$
$$C_6 = C_5 I_{xz} \quad (18)$$
$$C_7 = C_5(I_{zz} - I_{xx}) \quad (19)$$
$$C_8 = \frac{I_{xx}}{C_0} \quad (20)$$
$$C_9 = C_8(I_{xx} - I_{yy}) + C_2 I_{xz} \quad (21)$$

where I_{xx}, I_{yy}, I_{zz} are the diagonal components and I_{xz} is the x-z axis cross-component of the aircraft's inertia matrix I.

The forces and moments acting on the flight vehicle are mainly due to thrust provided by the aircraft's powerplant and aerodynamic forces and moments both from the motion of the aircraft and the current inputs to the aircraft's control surfaces. These forces and moments are given by the following equations:

$$F_x = T + \frac{1}{2}C_X\rho V^2 S \quad (22)$$
$$F_y = \frac{1}{2}C_Y\rho V^2 S \quad (23)$$
$$F_z = \frac{1}{2}C_Z\rho V^2 S \quad (24)$$
$$l = \frac{1}{2}C_l\rho V^2 Sb \quad (25)$$
$$M = \frac{1}{2}C_M\rho V^2 Sc \quad (26)$$
$$N = \frac{1}{2}C_N\rho V^2 Sb \quad (27)$$

where S, c, b are the aircraft's planform wing area, wing chord and wing span respectively, V is the total aircraft velocity and ρ is the atmospheric density of surrounding airflow. The thrust force T is approximated as:

$$T = \frac{P_{max}\eta}{V}\delta_T \quad (28)$$

where P_{max} is the maximum engine power available, η is the propeller efficiency and δ_T is the throttle control input to the aircraft. The force and moment coefficients $C_{X,Y,Z,l,M,N}$ are all functions of the current aircraft velocity and orientation and the control inputs $\delta_e, \delta_a, \delta_r$ from the elevator, ailerons and rudder respectively. These coefficients are evaluated using Equations (29) to (36) shown below:

$$C_L = C_{L_0} + C_{L_\alpha}\alpha + C_{L_q}\left(\frac{c}{2V}\right)q + C_{L_{\delta_e}}\delta_e \quad (29)$$
$$C_D = C_{D0} + KC_L^2 \quad (30)$$
$$C_X = C_D sin(\alpha) - C_L cos(\alpha) \quad (31)$$
$$C_Z = -C_D cos(\alpha) - C_L sin(\alpha) \quad (32)$$
$$C_Y = C_{Y_\beta}\beta + C_{Y_p}\left(\frac{b}{2V}\right)p + C_{Y_r}\left(\frac{b}{2V}\right)r + C_{Y_{\delta_a}}\delta_a + C_{Y_{\delta_r}}\delta_r \quad (33)$$
$$C_l = C_{l_\beta}\beta + C_{l_p}\left(\frac{b}{2V}\right)p + C_{l_r}\left(\frac{b}{2V}\right)r + C_{l_{\delta_a}}\delta_a + C_{l_{\delta_r}}\delta_r \quad (34)$$
$$C_M = C_{M_0} + C_{M_\alpha}\alpha + C_{M_q}\left(\frac{c}{2V}\right)q + C_{M_{\delta_e}}\delta_e + C_L\left(\frac{\delta_{cg}}{c}\right) \quad (35)$$
$$C_N = C_{N_\beta}\beta + C_{N_p}\left(\frac{b}{2V}\right)p + C_{N_r}\left(\frac{b}{2V}\right)r + C_{N_{\delta_a}}\delta_a + C_{N_{\delta_r}}\delta_r \quad (36)$$

where K is the lift-induced drag coefficient of the aircraft and α, β are the aircraft angle of attack and angle of

sideslip respectively. The parameters $C_{(.)_{(.)}}, K, \eta, P_{max}$ are aircraft specific model parameters that can be approximated as constants for most aircraft undertaking subsonic flight. These parameters are usually evaluated for an aerial vehicle as part of the control design process using a combination of empirical analysis and wind tunnel testing. The velocity (v_b) and rotation rates (ω_b) of the vehicle, referenced to the body frame are found by integrating equations (6-11) w.r.t time given the values in equations (12-36). The velocity (v_n) of the vehicle in the navigation frame of reference is found using the body to navigation frame transformation by:

$$v_n = C_b^n v_b \tag{37}$$

Equations (1) and (3) are then used to calculate the position and Euler angles of the vehicle.

2.3 Estimation Process

Configuration 1

In the first configuration the estimated state vector $\delta\hat{x}$ is composed of twelve inertial navigation errors; three velocity errors, three misalignments, three accelerometer errors and three gyro errors and the nine vehicle model errors in velocity, attitude and rotation rates.

$$\begin{aligned} \delta\hat{x}_{INS} &= [\delta v_{N_I}, \delta v_{E_I}, \delta v_{D_I}, \psi_N, \psi_E, \psi_D, \\ &\quad \delta f_{bx}, \delta f_{by}, \delta f_{bz}, \delta\omega_{bx}, \delta\omega_{by}, \delta\omega_{bz}] \quad (38) \\ \delta\hat{x}_{FVM} &= [\delta v_{N_V}, \delta v_{E_V}, \delta v_{D_V}, \delta\phi, \delta\theta, \delta\psi, \\ &\quad \delta p_v, \delta q_v, \delta r_v] \quad (39) \\ \delta\hat{x} &= [\delta\hat{x}_{INS}, \delta\hat{x}_{FVM}]^T \quad (40) \end{aligned}$$

The process model for the errors is expressed as:

$$\dot{\delta\hat{x}} = \mathbf{F}\delta\hat{\mathbf{x}} + \mathbf{G}\mu \tag{41}$$

where $\mathbf{F}$ describes the combined INS and FVM error dynamics, $\mathbf{G}$ is the noise input matrix and μ is an uncorrelated, zero-mean process noise vector of dimension 21 and covariance $\mathbf{Q}$ representing the inertial sensor and FVM process noises. The error dynamics matrix $\mathbf{F}$ is:

$$\mathbf{F} = \begin{bmatrix} \mathbf{F_{INS}} & 0 \\ 0 & \mathbf{F_{FVM}} \end{bmatrix} \tag{42}$$

$$\mathbf{F_{INS}} = \begin{bmatrix} 0 & A_n & C_b^n & 0 \\ 0 & 0 & 0 & -C_b^n \\ 0 & 0 & 0 & 0 \\ 0 & 0 & 0 & 0 \end{bmatrix} \tag{43}$$

$$A_n = \begin{bmatrix} 0 & -f_D & f_E \\ f_D & 0 & -f_N \\ -f_E & f_N & 0 \end{bmatrix} \tag{44}$$

where $f_{N,E,D}$ are the navigation frame components of the vehicle's specific force and $\mathbf{F_{FVM}}$ is calculated as the Jacobian of the non-linear FVM equations w.r.t the FVM states x_{FVM} as shown:

$$\begin{aligned} \dot{x}_{FVM} &= fn(x_{FVM}, U_{cont}) \quad (45) \\ \mathbf{F_{FVM}} &= \frac{\partial\dot{x}_{FVM}}{\partial x_{FVM}} \quad (46) \\ x_{FVM} &= [u, v, w, \phi, \theta, \psi, p, q, r] \end{aligned}$$

The noise input matrix $\mathbf{G}$ is:

$$\mathbf{G} = \begin{bmatrix} C_b^n & 0 & 0 & 0 & 0 & 0 \\ 0 & -C_b^n & 0 & 0 & 0 & 0 \\ 0 & 0 & I & 0 & 0 & 0 \\ 0 & 0 & 0 & I & 0 & 0 \\ 0 & 0 & 0 & 0 & I & 0 \\ 0 & 0 & 0 & 0 & 0 & I \end{bmatrix} \tag{47}$$

A virtual observation (z_{obs}) is made as the difference between the velocity and attitude predicted by the INS and FVM. The relationship between the estimated errors and observation is given by the observation model ($\mathbf{H}$):

$$\begin{aligned} z_{obs} &= \begin{bmatrix} v_{INS} - v_{FVM} \\ \Psi_{INS} - \Psi_{FVM} \end{bmatrix} \quad (48) \\ &= \mathbf{H}\delta\mathbf{x} + \nu \quad (49) \end{aligned}$$

$$\mathbf{H} = \begin{bmatrix} I & 0 & 0 & 0 & -I & 0 & 0 \\ 0 & B & 0 & 0 & 0 & -I & 0 \end{bmatrix} \tag{50}$$

$$B = \begin{bmatrix} -c_\psi sec_\theta & -s_\psi sec_\theta & 0 \\ s_\psi & -c_\psi & 0 \\ -t_\theta c_\psi & -t_\theta s_\psi & -1 \end{bmatrix} \tag{51}$$

where ν is an uncorrelated, zero-mean observation noise vector of dimension 6 and covariance $\mathbf{R}$ and $\Psi = [\phi, \theta, \psi]$ are the Euler angles as predicted by the INS.

A Kalman filter is then used to estimate the system errors from the virtual observations. Errors in the positions calculated by each system are not estimated due to an inherent un-observability in these states. This lack of observability stems from the lack of coupling between the position and other states in the FVM (i.e. forces acting on the aircraft not directly being a function of the aircraft's position). Usually a coupling could be attained through the variation in atmospheric density (ρ) with altitude or through operating over a large area of the Earth's surface where the navigation frame would rotate as a function of position, however the assumption is that these couplings would produce very weak observability at best.

Configuration 2

In the second configuration the estimated state vector is composed of errors in the acceleration and rotation rates as read from the inertial sensors and from the FVM, thus:

$$\begin{aligned}\delta\hat{x}_{IMU} &= [\delta f_{bx_I}, \delta f_{by_I}, \delta f_{bz_I}, \\ &\quad \delta\omega_{bx_I}, \delta\omega_{bx_I}, \delta\omega_{bx_I}] \quad (52)\\ \delta\hat{x}_{FVM} &= [\delta f_{bx_v}, \delta f_{by_v}, \delta f_{bz_v}, \\ &\quad \delta\omega_{bx_v}, \delta\omega_{bx_v}, \delta\omega_{bx_v}] \quad (53)\\ \delta\hat{x} &= [\delta\hat{x}_{IMU}, \delta\hat{x}_{FVM}]^T \quad (54)\end{aligned}$$

In this case the process model is of the dynamics of the errors within the inertial sensors and the FVM error dynamics. The combined error dynamics are:

$$\dot{\delta\hat{x}} = \mathbf{F}\delta\hat{\mathbf{x}} + \mu \quad (55)$$

$$\mathbf{F} = \begin{bmatrix} \mathbf{F_{acc}} & 0 & 0 \\ 0 & \mathbf{F_{gyro}} & 0 \\ 0 & 0 & \mathbf{F_{FVM_{6\times6}}} \end{bmatrix} \quad (56)$$

Where μ is a white noise vector of dimension 12 and covariance $\mathbf{Q}$. The sensor errors in this configuration are modelled as a first order Markov process with time constant τ:

$$\mathbf{F_{acc}} = \begin{bmatrix} -(1/\tau_{ax}) & 0 & 0 \\ 0 & -(1/\tau_{ay}) & 0 \\ 0 & 0 & -(1/\tau_{az}) \end{bmatrix} \quad (57)$$

$$\mathbf{F_{gyro}} = \begin{bmatrix} -(1/\tau_{gx}) & 0 & 0 \\ 0 & -(1/\tau_{gy}) & 0 \\ 0 & 0 & -(1/\tau_{gz}) \end{bmatrix} \quad (58)$$

The process model for the errors in the FVM accelerations and rotation rates errors ($\mathbf{F_{FVM_{6\times6}}}$) and is calculated by:

$$\mathbf{F_{FVM_{6\times6}}} = \begin{bmatrix} 0 & \mathbf{F_{f_b|\omega_b}} \\ 0 & \mathbf{F_{\omega_b}} \end{bmatrix} \quad (59)$$

$$\mathbf{F_{f_b|\omega_b}} = \frac{\partial \dot{\mathbf{f_b}}}{\partial \omega_\mathbf{b}} \quad (60)$$

$$\mathbf{F_{\omega_b}} = \frac{\partial \dot{\omega_\mathbf{b}}}{\partial \omega_\mathbf{b}} \quad (61)$$

where $\mathbf{F_{f_b|\omega_b}}$ and $\mathbf{F_{\omega_b}}$ are Jacobians of the non-linear FVM equations w.r.t the FVM accelerations and rotation rates. In this case $\mathbf{F_{f_b|\omega_b}}$ is evaluated using a numerical method in order to evaluate the rate of change of the body axes acceleration (f_b) for varying values of ω_b perturbed about the value calculated by the FVM.

A virtual observation (z_{obs}) is made as the difference between the readings of the accelerations and rotation rates of the aircraft from the inertial sensors and those predicted by the FVM.

$$\begin{aligned} z_{obs} &= \begin{bmatrix} f_{b_{INS}} - f_{b_{FVM}} \\ \omega_{b_{INS}} - \omega_{b_{FVM}} \end{bmatrix} \quad (62)\\ &= \mathbf{H}\delta\mathbf{x} + \nu \quad (63)\end{aligned}$$

Figure 4: The Brumby MkIII UAV

$$\mathbf{H} = \begin{bmatrix} I & 0 & -I & 0 \\ 0 & I & 0 & -I \end{bmatrix} \quad (64)$$

where ν is an uncorrelated, zero-mean observation noise vector of dimension 6 and covariance $\mathbf{R}$.

As in the first configuration, a Kalman filter is used to estimate inertial sensor and FVM errors from virtual observations.

3 Simulation Description

In this section we consider a scenario in which a aircraft using a GPS aided INS loses satellite transmission and can no longer provide positioning fixes to the INS. In this situation, errors in the INS pose estimate will grow without bound until a GPS fix is reacquired. The aircraft considered is shown in Figure (4). It is a small UAV weighing 40kg with a wing span of 2.8 meters, capable of flying at 100kts. Vehicle acceleration and rotation rates are read from and onboard low-cost strapdown IMU for which specifications are shown in Table 1. All vehicle

Sampling Rate	$400Hz$
Accelerometer Noise	$0.1m/s^2$
Gyro Noise	$0.1deg/s$
Accelerometer Bias Stability	$\pm0.1m/s^2$
Gyro Bias Stability	$\pm0.1deg/s$

Table 1: Strapdown IMU Specifications

model parameters for the UAV, as used by equations (6-36), are known a-priori. Such vehicle model parameters, necessary for autonomous control of the UAV, are often known to an accuracy of $\pm5\%$ of the true values. In our simulation, the onboard vehicle navigation system starts to aid the INS with the FVM information at the time of satellite signal loss. Two simulations are run

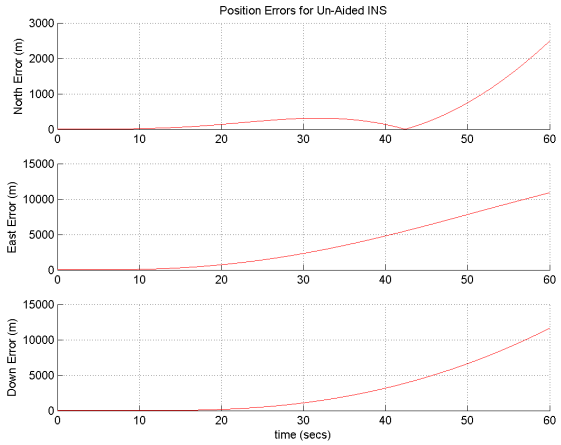

Figure 5: Absolute Position Errors for the Un-Aided INS

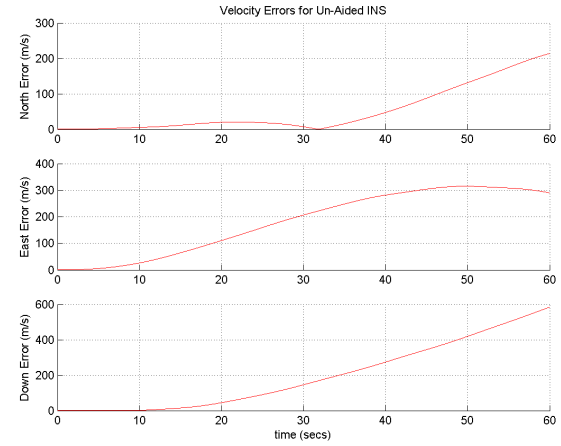

Figure 6: Absolute Velocity Errors for the Un-Aided INS

for each of the two configurations shown in Figures (1) and (2), the first in which all of the vehicle model aerodynamic parameters $C_{(.)_{(.)}}$ are varied by random errors within $\pm 5\%$ of their true values and the second in which the parameters are varied by $\pm 20\%$. In the scenario the UAV continues along it's flight path as designated by it's current mission, which in this case is to track moving features on the ground. Small perturbations are applied to the UAV's controls such that the vehicle undergoes a small amplitude Dutch roll behavior. This motion is critical to the operation of the combined navigation system as it excites the coupling in the error dynamics of the FVM, providing observability of all of the estimated error sources.

4 Results

This section presents the results from the simulation. Figures (5), (6) and (7) show the errors in the un-aided

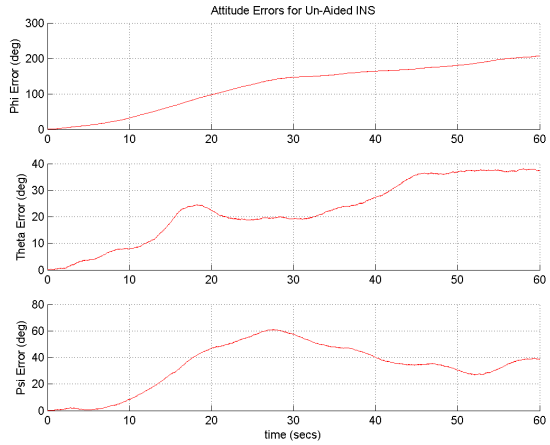

Figure 7: Absolute Euler Angle Errors for the Un-Aided INS

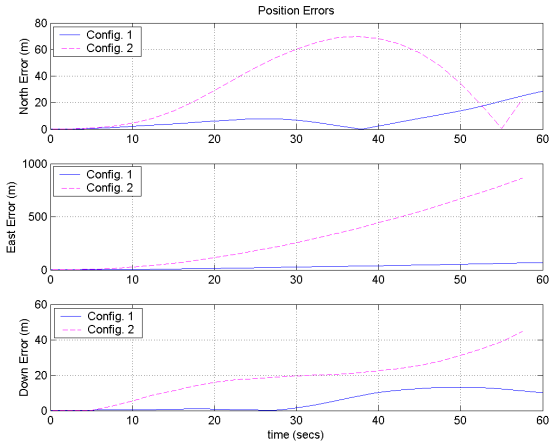

Figure 8: Absolute Position Errors with FVM Aiding: $\pm 5\%$ Parameter errors

INS vehicle position, velocity and Euler angles. The errors are considerable even over a short amount of time and are attributed mainly to the biases in the IMU readings. Figures (8), (9) and (10) show the estimated position, velocity and Euler angles of the vehicle when the two different configurations for vehicle model aiding are applied to the navigation system, with vehicle model parameter errors of $\pm 5\%$. Figures (11), (12) and (13) show the estimated position, velocity and Euler angles of the vehicle when the two different configurations with vehicle model parameter errors of $\pm 20\%$. The first configuration exhibits a lower error than the second configuration in both modelling error cases, particularly when modelling errors are large and the performance of configuration 2 is severely diminished. When vehicle model errors are large in the second configuration, cross-coupling in the rota-

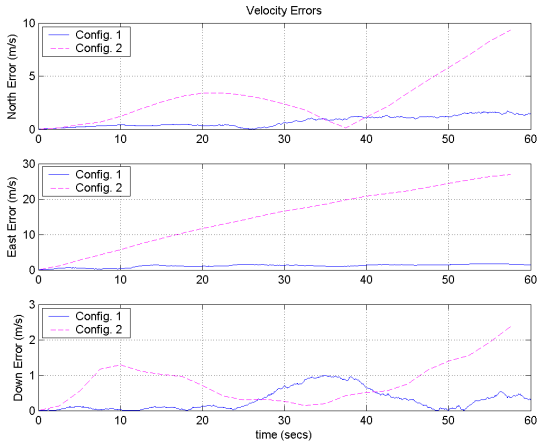

Figure 9: Absolute Velocity Errors with FVM Aiding: ±5% Parameter errors

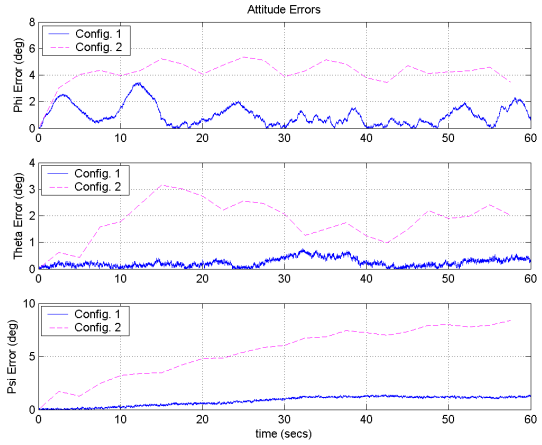

Figure 10: Absolute Euler Angle Errors with FVM Aiding: ±5% Parameter errors

tion rate and acceleration errors in the FVM cause poor accelerometer bias estimates, thus reducing the position and velocity accuracies. The advantage of the first configuration is that there is only a marginal loss in accuracy between the ±5% and ±20% modelling error cases. This robustness to modelling errors stems from the fact that FVM errors will result in slow error growth in the velocity and attitude that can be estimated and rejected with greater ease than the rapid error dynamics in acceleration and rotation rates, associated with FVM parameter errors. Similar results can be seen in the IMU bias estimates from each configuration as shown in Figures (14) to (17).

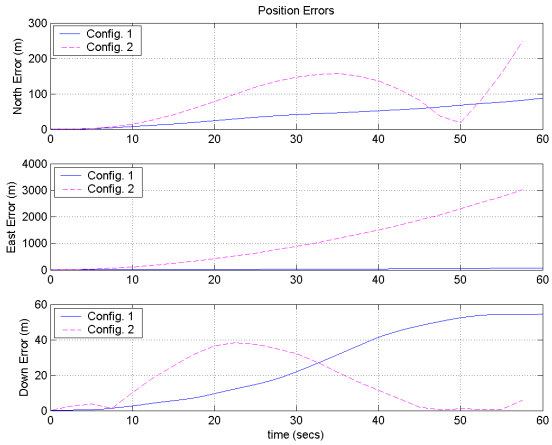

Figure 11: Absolute Position Errors with FVM Aiding: ±20% Parameter errors

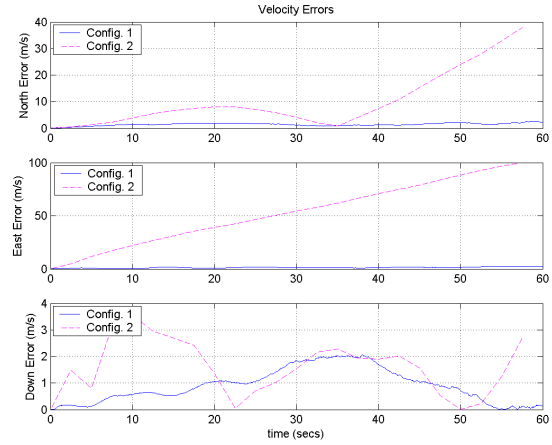

Figure 12: Absolute Velocity Errors with FVM Aiding: ±20% Parameter errors

5 Conclusions and Future Work

This paper has demonstrated two different methods for aiding the solution of an INS using vehicle model information for an aerial vehicle in simulation. It has been shown in the simulation results that the navigation system performance (reduction in position, velocity and Euler angle errors) has been significantly increased from the un-aided system when vehicle model information is applied. We have shown that the combined navigation system performance is still greater than the un-aided INS, even when there exists small parameter errors in our model, particular when aiding using configuration 1. In the presence of parameter errors, it has been shown that the second configuration is less sucsessful at estimating IMU biases than the first configuration. This is most likely due to parameter errors resulting in sudden

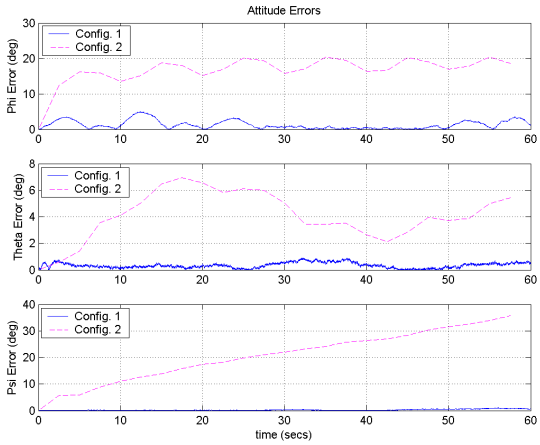

Figure 13: Absolute Euler Angle Errors with FVM Aiding: ±20% Parameter errors

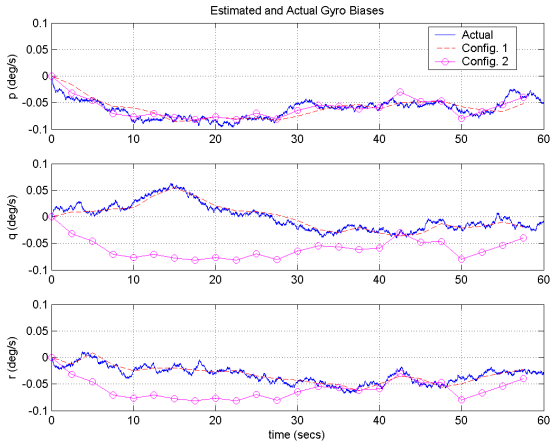

Figure 15: Actual and Estimated Gyro biases with FVM Aiding: ±5% Parameter errors

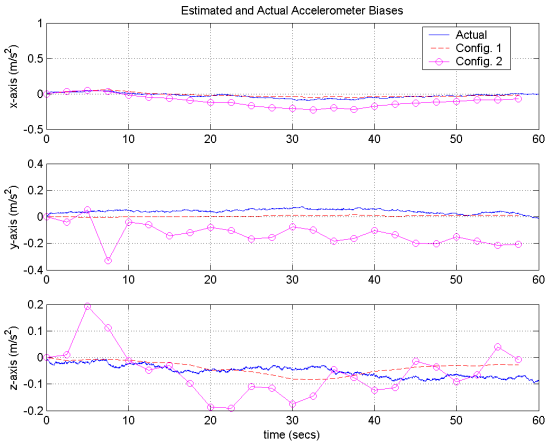

Figure 14: Actual and Estimated Accelermometer biases with FVM Aiding: ±5% Parameter errors

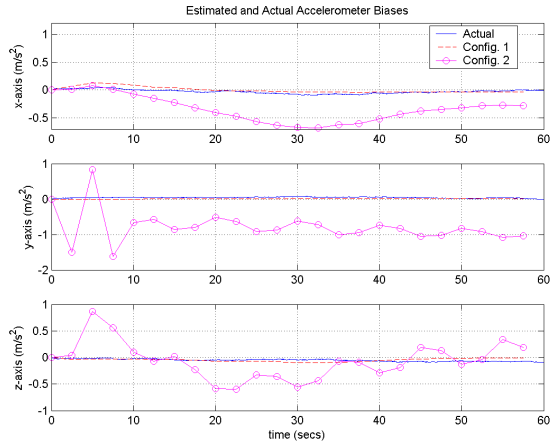

Figure 16: Actual and Estimated Accelermometer biases with FVM Aiding: ±20% Parameter errors

acceleration errors in the FVM but only gradual, slowly growing errors in the FVM velocity and Euler angles. One solution to this may be to not attempt to estimate accelerometer biases when it is known that the vehicle model parameters of the flight vehicle are inaccurate, estimating only the gyro biases.

In future work we propose to study the relationship between UAV manoeuvres and observability of the FVM dynamic errors, such as to determine exactly which aircraft control actions will ensure observability of the error estimates. Future work will also look at applying the FVM aiding navigation system to a real flight vehicle in which unknown wind disturbances and parameter errors will pose significant challenges to the system design.

Acknowledgments

This work is supported in part by the ARC Centre of Excellence programme, funded by the Australian Research Council (ARC) and the New South Wales State Government.

References

[Sukkarieh et al., 1999] S. Sukkarieh, E.M. Nebot, H.F. Durrant-Whyte, "A high integrity IMU/GPS navigation loop for autonomous land vehicle applications," IEEE Trans. on Robotics and Automation, Vol 15, No. 3, pp. 572-578, June 1999.

[Meyer-Hilberg and Jacob, 1994] J. Meyer-Hilberg, T. Jacob, "High accuracy Navigation and Landing System using GPS/IMU System Integration," IEEE Po-

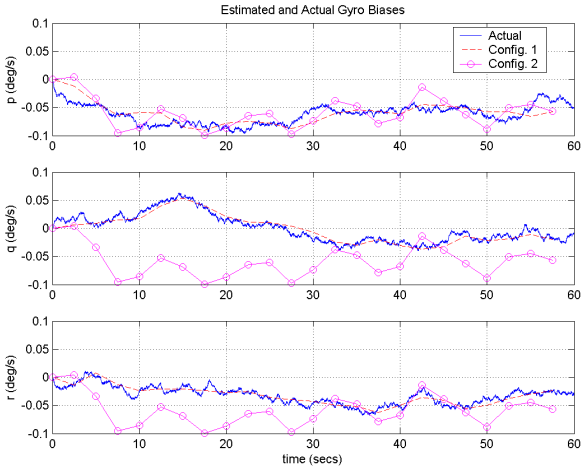

Figure 17: Actual and Estimated Gyro biases with FVM Aiding: ±20% Parameter errors

sition, Location and Navigation Symposium, April 1994.

[Yang et al., 2000] Y. Yang, J. Farrell, M. Barth, "High-Accuracy, High-Frequency Differential Carrier Phase GPS aided low-cost INS," IEEE Position, Location and Navigation Symposium, March 2000.

[Bar-Itzhack, 1978] I.Y. Bar-Itzhack, "Optimal Updating of INS Using Sighting Devices," AIAA Journal of Guidance and Control, Vol 1, No. 5, pp. 305-312, October, 1978.

[Kim and Sukkarieh, 2003] J.H. Kim, S. Sukkarieh, "Airborne Simultaneous Localization and Map Building," IEEE International Conference on Robotics and Automation, Taipei, 2003

[Ma et al., 2003] M. Xin, S. Sukkarieh, J.H. Kim, "Vehicle Model Aided Inertial Navigation," IEEE Conference on Intelligent Transportation Systems, Shanghai, China 2003.

[Koifman and Bar-Itzhack, 1999] M. Koifman, I.Y. Bar-Itzhack, "Inertial Navigation System aided by Aircraft Dynamics," IEEE Trans. on Control Systems Technology, Vol. 7, No. 4, pp. 487-493, July 1999.

[Dissanayake et al., 2001] M.W.M.G. Dissanayake, S. Sukkarieh, E.M. Nebot, H.F. Durrant-Whyte "The Aiding of a Low-Cost Strapdown Inertial Measuring Unit Using Vehicle Model Constraints for Land Vehicle Applications," IEEE Trans. on Robotics and Automation, Vol. 17, No. 5, pp. 731-747, October 2001.